Ferroelectrics, 387:189–196, 2009

ISSN: 0015-0193 print / 1563-5112 online
DOI: 10.1080/00150190902967097

The Effect of Impurity Phases on the Structure and Properties of Microwave Dielectrics Based on Complex Perovskites $Ba(Co^{2+}_{1/3}Nb_{2/3})O_3$

O. OVCHAR,[1,*] A. BELOUS,[1] O. KRAMARENKO,[1]
D. MISCHUK,[1] B. JANCAR,[2] M. SPREITZER,[2] D. SUVOROV,[2]
G. ANNINO,[3] D. GREBENNIKOV,[4] AND P. MASCHER[4]

[1]V.I. Vernadskii Institute of General and Inorganic Chemistry NAS of Ukraine, 32/24 Palladin ave., Kyiv-142, 03680, Ukraine
[2]Jozef Stefan Institute, Jamova 39, 1000, Ljubljana, Slovenia
[3]Istituto per i Processi Chimico-Fisici, CNR., via G. Moruzzi 1, 56124 Pisa, Italy
[4]McMaster University, Hamilton, Ontario, L8S 4K1, Canada

Two major secondary phases have been revealed in the ceramics based on the complex perovskites $Ba(Co_{1/3}Nb_{2/3})O_3$: a Ba-rich compound $Ba_8CoNb_6O_{24}$ with the layered perovskite structure, and a Nb-rich compound with the structure of tetragonal tungsten bronze and the composition close to $Ba_6CoNb_9O_{30}$. The presence of a small amount of the Ba-rich phase is accompanied with the rise in the quality factor (Q) of the material whereas the high amount is deleterious to Q. In contrast, the presence of even a small amount of Nb-rich phase always results in a sharp fall in the Q-factor. The ways of tuning temperature coefficient τ_f in $Ba(Co_{1/3}Nb_{2/3})O_3$ ceramics have been discussed.

Keywords Dielectrics; complex perovskites; cation ordering; impurities; quality factor

1. Introduction

Complex barium tantalates and niobates $Ba(A^{2+}_{1/3}B^{5+}_{2/3})O_3$ (A^{2+} = Mg, Co, Zn; B^{5+} = Ta, Nb) with the perovskite structure have found numerous applications in modern communications as the materials for dielectric resonators with extremely high quality factor (*Q*-factor) in the microwave (MW) frequency range [1–3]. Among these materials $Ba(Ta_{1/3}Mg_{2/3})O_3$ perovskites demonstrate the product $Q \times f$ as high as 300 000 GHz in the centimeter wavelength band [2]. These extremely high values of the *Q*-factor are generally ascribed to the formation of the 1:2 ordered B-subblatice of a perovskite $Ba(A^{2+}_{1/3}B^{5+}_{2/3})O_3$, which comprises single layers of A^{2+} cations alternating with double layers of B^{5+} cations perpendicular to the <111> direction of the pseudocubic cell [4–6]. Various authors have recently shown that the ordering processes in $Ba(A^{2+}_{1/3}B^{5+}_{2/3})O_3$ can be promoted through the local structural changes which are initiated by either ZnO evaporation in $Ba(Zn_{1/3}Ta_{2/3})O_3$ (BZT) and

Received November 1, 2008; in final form February 6, 2009.
*Corresponding author. E-mail: ovcharoleg@yahoo.com

$Ba(Zn_{1/3}Nb_{2/3})O_3$ (BZN), or introducing aliovalent ions (for instance Zr^{4+}) in the structure, or slight shifting from stoichiometric cation ratio [5, 6]. Apparently, these changes may involve the formation of microstructural defects, or secondary phases in the 1:2 perovskite matrixes, which consecutively contribute to the dielectric properties of the sintered materials. Therefore, much attention has been focused to the role of the microstructure of $Ba(A^{2+}_{1/3}B^{5+}_{2/3})O_3$ in the attainment of the highest $Q\times f$ products [6–8]. For instance, the formation of $Ba_5Ta(Nb)_4O_{15}$, $BaTa(Nb)_2O_6$, $Ba_8ZnTa(Nb)_6O_{24}$, $Ba_8CoNb_6O_{24}$, $BaNb_6O_{16}$ have been reported by several authors in various complex 1:2 perovskites [5, 7–9]. The majority of these secondary phases were assigned to the factors deteriorating the *Q*-factor. However, the reported data are not presented systematically, and do not explain the big scatter in dielectric parameters, which is the most visible in the niobate-based materials. Therefore, in this paper, we will try to summarize our recent findings with respect to the formation of secondary phases in the perovskites $Ba(Co^{2+}_{1/3}Nb_{2/3})O_3$ (BCN) with non-stoichiometric compositions as well as the influence of the secondary phases on the microwave dielectric properties of the studied materials.

2. Experimental Procedure

In this work both A-site and B-site non-stoichiometric compositions of the perovskites $Ba(Co_{1/3}Nb_{2/3})O_3$ have been studied. The ceramics were produced by the two-step mixed-oxide route described elsewhere [10]. The starting reagents were extra pure Co_3O_4 (99.95%), Nb_2O_5 (99.9%), and $BaCO_3$ (99.9%). At the first stage the corresponding columbites $Co_{1+x}Nb_2O_6$ were synthesized from the weighted mixtures Co_3O_4-$3Nb_2O_5$ by calcining them at 1150°C for 4 hours. At the second stage, the appropriate ratios of $BaCO_3$ and the corresponding columbite were ball milled again, and calcined at 1150°C for another 4 hours. In contrast, the individual phases $Ba_8CoNb_6O_{24}$ and $Ba_6CoNb_9O_{30}$ have been produced from the same reagents by a single-step calcinations procedure. The sintering was performed in air for 8 hours at the temperatures 1350°C–1500°C. The phase composition and crystal lattice parameters of the sintered ceramics were examined by means of X-ray diffraction analysis (XRD) using CuKα - radiation (Model PW 1700, Philips, Eindhoven, The Netherlands). Microstructural analysis of the ceramic samples was performed by means of scanning electron microscopy (JEOL, JSM 5800, Tokyo, Japan) using energy dispersive X-ray spectroscopy (EDX) and the LINK software package (ISIS 3000, Oxford Instruments, Bucks, UK). Electron diffraction studies and TEM microscopic investigations of the foils were performed using a transmission electron microscope (JEOL 2000FX, JEOL, Tokyo, Japan) operating at 200 kV. Raman spectra were taken at room temperature on a Renishaw 2000 spectrometer. 514nm line of Ar^+ ion laser was used as an excitation source. The dielectric characteristics of the materials (ε, Q, and τ_f) at frequencies around 10 GHz were examined using a cavity reflection method on the Network Analyser PNA-L Agilent N5230A. In addition, the quality factor of the studied materials was examined within the frequency range of 40–70 GHz by means of Whispering Gallery Mode (WGM) technique by a millimeter wave vector analyzer model 8-350-2 (courtesy of AB millimetre, Paris, France).

3. Results and Discussion

Co-deficient BCN

The variation in Co-deficiency in the system $Ba_3Co_{1+x}Nb_2O_9$ corresponded to $-0.15 \leq x \leq 0$. According to the XRD and SEM analyses of sintered samples a Ba-rich impurity phase

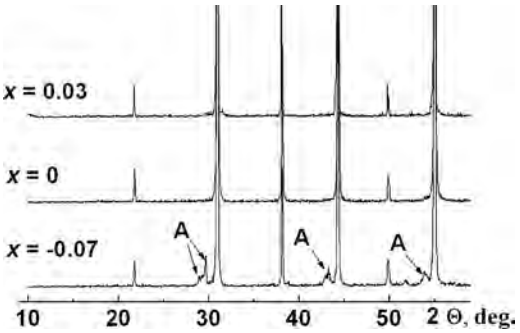

Figure 1. XRD patterns collected on the crushed powder of the samples $Ba_3Co_{1+x}Nb_2O_9$ with different composition sintered at 1470°C for 8 hours. A- $Ba_8CoNb_6O_{24}$.

starts to form at $x \leq -0.05$. Its amount increases with increasing Co-deficiency (Fig. 1). Both XRD and EDS microstructural analysis of the sampleswith the nominal composition $x = -0.15$ indicate the existence of secondary phase $Ba_8CoNb_6O_{24}$ with the layered structure of hexagonal perovskite which–as observed by SEM- exhibits the elongated grain morphology with the length exceeding 20 μm [11]. This structure adopts eight-layer stacking sequences with corner-sharing oxygen octahedra. Its main feature consists in the presence of strictly ordered layers of Co^{2+} cations separated by 1.88 nm, and the vacant-site layers [10]. In contrast to the results of the Ref. 10, in our study the dense ceramics $Ba_8CoNb_6O_{24}$ sintered at 1450°C for 8 hours did represent a multiphase composition comprising phases with slightly different Co content (Fig. 2). In the Co-deficient BCN the hexagonal perovskite phase starts nucleation at the grain boundaries (Fig. 3a). In the ceramics sintered for 8 hours some grain boundaries contain two regions with the different crystal structures: 1:2 ordered cubic perovskite $Ba_3CoNb_2O_9$ (A in the Fig. 3a and b), and layered perovskite $Ba_8CoNb_6O_{24}$ (B in the Fig. 3a and b). These regions are separated by the mixed-structure field (C in the Fig. 3a and b). However, the layered perovskite regions (B) do not yet demonstrate a presence of the strict 8-layer stacking sequences (Fig. 3c). These data may probably indicate the formation of different isostructural derivatives of $Ba_8CoNb_6O_{24}$

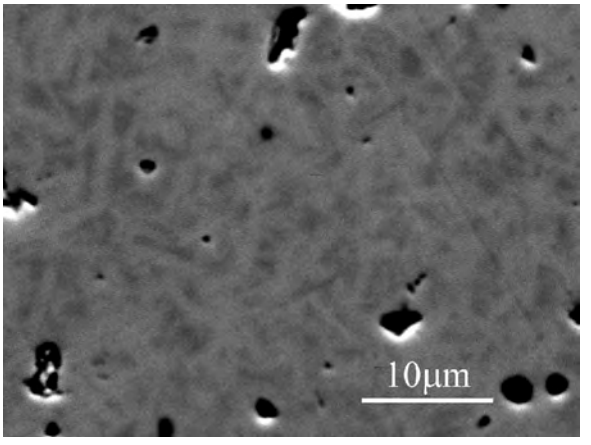

Figure 2. SEM microphotograph of the polished surface of $Ba_8CoNb_6O_{24}$.

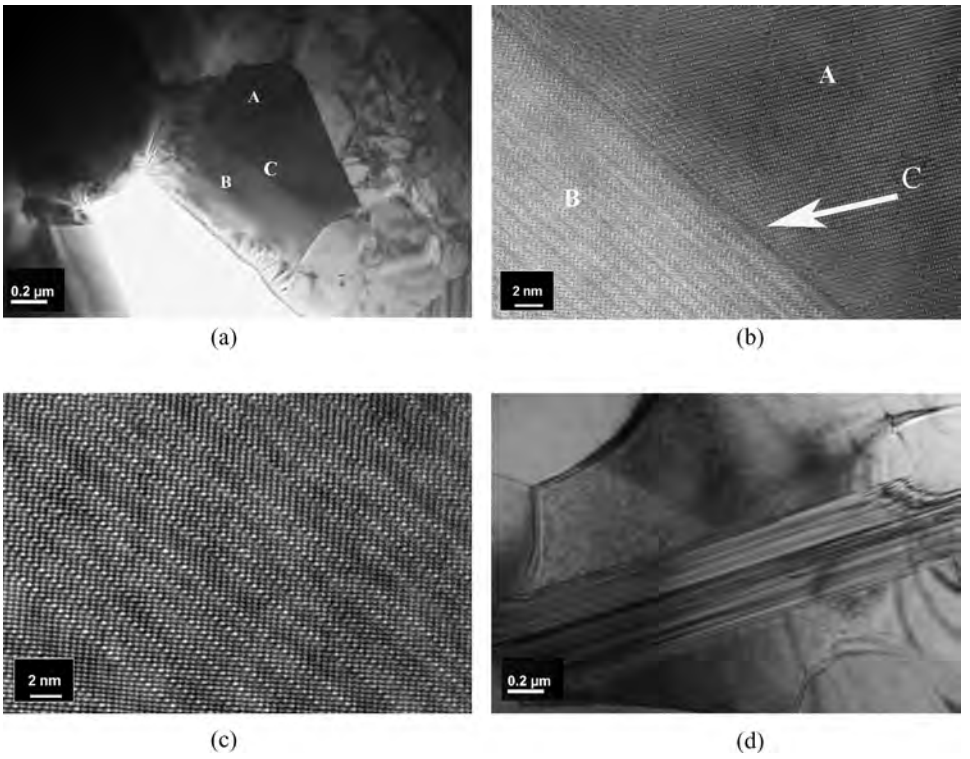

Figure 3. TEM images of the grain boundary regions of $Ba_3Co_{1+x}Nb_2O_9 (x = -0.15)$ displaying the areas with the different crystal structure (A, B, C) located on a single grain (a,b), stacking sequences of the layered hexagonal perovskite (c), and inclusions of layered perovskite along the BCN grains (d).

with the close chemical compositions but different stacking motives. However, this requires further analysis.

Analysis of the microwave dielectric properties of the materials $Ba_3Co_{1+x}Nb_2O_9$ measured at around 10 GHz denotes only slight variation of the permittivity within the range of 32–34 with changing Co content. In contrast, the magnitude of the Q-factor passes through the maximum in the Co-deficient samples resulting in the increase in the product $Q \times f$ from 55 000–60 000 GHz up to around 85 000–90 000 GHz within the range $-0.07 \leq x \leq -0.05$ (Fig. 4), which corresponds to the multiphase compositions. The WGM characterization of the sintered materials in the millimeter wavelength band (50–70 GHz) indicates a similar behavior of the Q-factor (Fig. 4a). Moreover, at $x = -0.07$ the $Q \times f$ reaches values higher than 100 000 GHz from which one can estimate the contribution of extrinsic sources (including structural distortions, secondary phases, grain boundaries and micropores) into the dielectric loss as at least 20%. The observed increase in the Q-factor in the Co-deficient BCNs correlates with the corresponding increase in the 1:2 ordering degree found from the TEM electron diffraction data and the Raman spectra which are not presented here because of the page limits. This means that exactly improved ordering is responsible for higher Q values observed in the non-stoichiometric BCNs. As stated above, increasing Co-deficiency at $x \leq -0.05$ resulted in the formation of secondary phase $Ba_8CoNb_6O_{24}$, which is accompanied by the reduction in Q (Fig. 4a). According to the Ref. 10, the Q-factor of

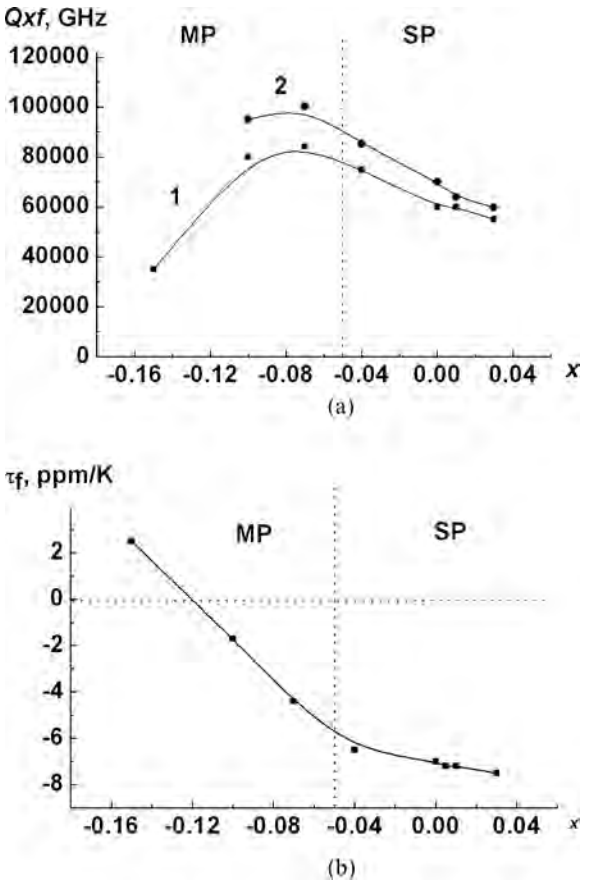

Figure 4. *Qxf* product (a) and the temperature coefficient of resonant frequency (τ_f) (b) of the samples $Ba_3Co_{1+x}Nb_2O_9$ as a function of Co content measured at the frequencies of around 10 GHz (1) and 60 GHz (2); MP-multiphase region, SP-single-phase region.

the strictly ordered $Ba_8CoNb_6O_{24}$ significantly depends on the processing conditions, and the best measured product *Qxf* of the sample sintered at 1500°C for 12 hours was as high as 53000 GHz at the frequency 3 GHz. In this study, the product *Qxf* of $Ba_8CoNb_6O_{24}$ ceramics was higher, and exceeded 100 000 GHz at the frequencies of around 10 GHz . Although this phase exhibits high enough microwave dielectric parameters (Q is higher than that of BCN), its increasing amount monotonically deteriorates the Q-factor of the multiphase material. The reason can be due to the increasing number of microstructural defects arising with the growth of $Ba_8CoNb_6O_{24}$ inclusions along the BCN grains (Fig. 3d). However, this effect is negligible in the case of small-size precipitates of $Ba_8CoNb_6O_{24}$ (which are observed when the deviation from compositional stoichiometry is small), and the maximum Qs are attained in the multiphase compositions at $x \leq -0.05$ (Fig. 4a) .

Besides the reduced Q-factor of a non-stoichiometric BCN, we have found much more positive effect of the $Ba_8CoNb_6O_{24}$ on the temperature coefficient of resonant frequency (τ_f) of multiphase material: τ_f changes its sign with the increasing concentration of $Ba_8CoNb_6O_{24}$ within the range $-0.15 \leq x \leq -0.1$ (Fig. 4b). This fact can be attributed to the opposite signs of τ_f in the individual impurity phase $Ba_8CoNb_6O_{24}$ ($\tau_f = +\ 12$

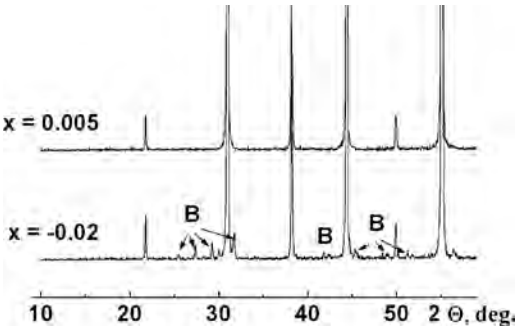

Figure 5. XRD patterns collected on the crushed powder of the samples $Ba_{3+3x}CoNb_2O_9$ with different composition sintered at 1470°C for 8 hours. B- $Ba_6CoNb_9O_{30}$.

ppm/K) and matrix BCN ($\tau_f = -7$ ppm/K). As a consequence, the volume temperature compensation effect appears at a certain ratio of constituting phases in the Co-deficient BCN. This allows an obtainment of temperature stable dielectrics with high quality factor of around 80 000 GHz simply by a proper adjustment of Co concentration.

Ba-deficient BCN

In the system $Ba_{3+3x}CoNb_2O_9$ the compositions corresponded to $-0.1 \leq x \leq 0$. In this system, even at small negative x a Nb-rich impurity phase appears with the peaks corresponding to $Ba_6CoNb_9O_{30}$ (PDF # 73-1879) (Fig. 5). EDS analysis of the Nb-rich phase, which is abundant in the samples with the highest Ba-deficiency ($x = -0.1$), has shown its composition to be close to the $Ba_6CoNb_9O_{30}$. This compound has been reported to have the structure of tetragonal tungsten bronze, and exhibit ferroelectric properties at room temperature [12]. In this study we have synthesized individual compound with the composition 6BaO -CoO -4.5Nb_2O_5 ($Ba_6CoNb_9O_{29.5}$), of which the sintered ceramics exhibited almost single-phase composition with small inclusions of the perovskite BCN phase. The $Ba_6CoNb_9O_{29.5}$ sample was melted at the temperatures of around 1400°C, well below the sintering temperature of BCN. Therefore, when the Ba-deficient BCN samples are sintered at higher temperatures the liquid phase $Ba_6CoNb_9O_{29.5}$ is distributed between the grains of the ceramics.

The dielectric properties of $Ba_6CoNb_9O_{29.5}$ have been measured over the wide frequency and temperature ranges. It demonstrated a strong dielectric relaxation within the frequency range of 10^3–10^6 Hz with the permittivity $\varepsilon = 350$ and dielectric loss tangent tg $\delta \approx 10^{-2}$ at 10^6 Hz. However, we revealed no phase transitions from room temperature up to the temperatures around 500°C. The temperature coefficient of permittivity (τ_ε) measured at 10^6 Hz was around -2000 ppm/K. In the microwave range, the dielectric loss of the sintered material was too high to allow a correct estimation of dielectric parameters. According to the measured data, the presence of $Ba_6CoNb_9O_{29.5}$ impurities would apparently deteriorate the quality factor of the sintered material. In fact, with a slight deviation from the stoichiometric composition, the amount of $Ba_6CoNb_9O_{29.5}$ is negligible, and the permittivity of the sintered materials varies only slightly within the range of $\varepsilon = 30$–33. At the same time, the magnitude of the Q-factor undergoes a rapid drop with the increasing Ba-deficiency (Fig. 6). It means exactly that the presence of the above impurity, even being

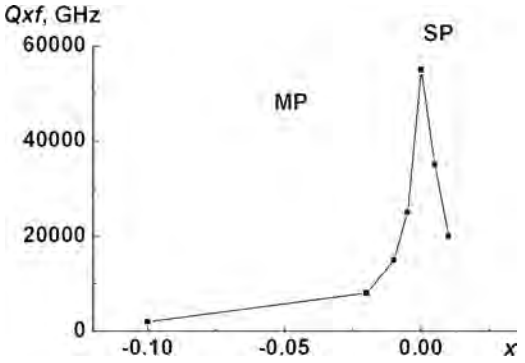

Figure 6. $Q\times f$ product of the samples $Ba_{3+3x}CoNb_2O_9$ as a function of Ba content measured at the frequency 10 GHz; MP-multiphase region, SP-single-phase region.

added in small quantities, gives the strongest contribution to the dielectric loss of BCN perovskites.

4. Conclusions

Two major impurity phases can be presented in the BCN ceramics depending on the chemical composition: the Ba-rich phase $Ba_8CoNb_6O_{24}$ with the layered perovskite structure in Co-deficient BCN, and the Nb-rich phase with the structure of tetragonal tungsten bronze phase and the composition close to $Ba_6CoNb_9O_{30}$ in Ba-defficient BCN. The quality factor was reduced in both cases with Co-deficient and Ba-deficient compositions around the stoichiometric $Ba(Co_{1/3}Nb_{2/3})O_3$. However, the reasons for the observed decrease in the $Q\times f$ are different. In the Ba-deficient BCN even a small concentration of Nb-rich phase $Ba_6CoNb_9O_{30}$ leads to a rapid fall of the product $Q\times f$. At the same time, when the concentration of the Ba-rich phase $Ba_8CoNb_6O_{24}$ in the Co-deficient BCN is law, the small-size inclusions of this phase do not deteriorate the $Q\times f$ of the sintered materials. However, the relatively high concentration of $Ba_8CoNb_6O_{24}$ probably initiates the formation of the grain boundary defects, which consecutively results in the decrease in the $Q\times f$. Moreover, the presence of the hexagonal perovskite $Ba_8CoNb_6O_{24}$ in the Co-deficient BCN allows the compensation of the negative temperature coefficient of resonant frequency of the BCN matrix without significant penalty in its quality factor.

Acknowledgements

This work was partially supported by the NATO Grant under the NATO SfP project 980881: "Dielectric Resonators" of the NATO "Science for Peace" Program.

References

1. S. Kawashima, M. Nishida, I. Ueda, H. Ouchi, and S. Hayakawa, Dielectric properties of $Ba(Zn,Ta)O_3$ –$Ba(Zn,Nb)O_3$ ceramic. *Proc. Ferroelect. Mater. Applicat.* **1**, 293–296 (1977).
2. H. Matsumoto, H. Tamura, and K. Wakino, $Ba(Mg,Ta)O_3$-$BaSnO_3$ High-Q Dielectric Resonator. *Jpn. J. Appl. Phys.* **30**, 2347–2349 (1991).

3. H. Hughes, D.M. Iddles, and I. M. Reaney, Niobate-based microwave dielectrics suitable for third generation mobile phone base stations. *Appl. Phys. Letters*. **79**(18), 2952–2954 (2001).
4. F. Galasso and J. Pyle, Ordering in Compounds of the $A(B'_{0.33}Ta_{0.67})O_3$ Type. *Inorg. Chem.* **2**(3), 482–484 (1963).
5. S. Desu and H. M. O'Bryan, Microwave loss quality of $Ba(Zn_{1/3}Nb_{2/3})O_3$. *J. Am. Ceram. Soc.* **68**(10), 546–551 (1985).
6. P. K. Davis, J. Tong, and T. Negas, Effect of ordering-induced domain boundaries on low-loss $Ba(Zn_{1/3}Ta_{2/3})O_3$–$BaZrO_3$ perovskite microwave dielectrics. *J. Am. Ceram. Soc.* **80**(7), 1724–1740 (1997).
7. C.-W. Ahn, H.-J. Jang, S. Nahm, H.-M. Park, and H.-J. Lee, Effect of microstructure on the microwave dielectric properties of $Ba(Co_{1/3}Nb_{2/3})O_3$ and $(1-x)Ba(Co_{1/3}Nb_{2/3})O_3$–$xBa(Zn_{1/3}Nb_{2/3})O_3$ solid solutions. *J. Eur. Ceram. Soc.* **23**, 2473–2478 (2003).
8. K. Endo, K. Fujimoto, and K. Murakawa, Dielectric properties of ceramics in $Ba(Co_{1/3}Nb_{2/3})O_3$–$Ba(Zn_{1/3}Nb_{2/3})O_3$ solid solutions. *J. Am. Ceram. Soc.* **70**(9), C-215–C-218 (1987).
9. F. Azough, C. Leach, and R. Freer, Effect of nonstoichiometry on the structure and microwave dielectric properties of $Ba(Co_{1/3}Nb_{2/3})O_3$ ceramics. *J. Eur. Ceram. Soc.* **26**(14), 2877–2884 (2006).
10. T. V. Kolodiazhnyi, A. Petric, G. P. Johari, .and A. G. Belous, Effect of preparation conditions on cation ordering and dielectric properties of $Ba(Mg_{1/3}Ta_{2/3})O_3$ ceramics. *J. Eur. Ceram. Soc.* **22**(12), 2013–2021 (2002).
11. P. M. Mallinson, M. M. Allix, J. B. Claridge, R. M. Ibberson, D. M. Iddles, T. Price, and M. J. Rosseinsky, $Ba_8CoNb_6O_{24}$: a d^0 dielectric oxide host containing ordered d^7 cation layers 1.88 nm apart. *Angew. Chem. Int. Ed. Engl.* **44**(47), 7733–1136 (2005).
12. M. C. Foster, G. R. Brown, R. M. Nielson, and S. C. Abrahams, $Ba_6CoNb_9O_{30}$ and $Ba_6FeNb_9O_{30}$: Two New Tungsten-Bronze-Type-Like Ferroelectrics. *J. Appl. Cryst.* **30**, 495–501 (1997).